

Fluidized Bed Heat Exchanger where its temperatures are reduced. The cooled ash particles are then returned to combustor for generation of gas. Rotary blowers located below the cyclone and Fluidized Bed Heat Exchanger are also called positive displacement pump comprises casing, rotors and suction and discharge ducts. The number of rotating lobes in the blower can vary from two to four lobes based on pressure ratios and flow quantity. Depending upon operating speed and pressure ratio, the efficiency of rotary blower can be obtained through the nomograms.

The efficiency point will rise with the increasing boost and will move towards right over increase in blower speed. It can be seen that, at moderate speed and low boost, the efficiency of the blower will be over 90%. In this zone, the rotary blowers are normally to be operated. Boost is given in terms of pressure ratio, which is the ratio of absolute air pressure before the blower to the absolute air pressure after compression by the blower.

If no boost is present, the pressure ratio will be 1.0 means outlet pressure is equals to inlet pressure. For the reference boost, that is slightly above a pressure ratio of 2.0 compared to atmospheric pressure the efficiency of rotary blowers are in the range of 50% - 58%. Replacing a smaller blower with a larger one moves the point to the left means that it falls in higher efficiency areas. These rotary blowers are so rugged machines which makes very noisy and inefficient in nature. In general, the noise levels are more than 110 dB (at 10m), and the efficiency is less than 65% level.

Moreover, the characteristic curves run very steep; i.e., nearly constant volume flow is produced over a wide range of pressure ratio. Thus, to control the flow

rates at the same pressure ratio is difficult and requires design changes in lobes/rotors profiles.

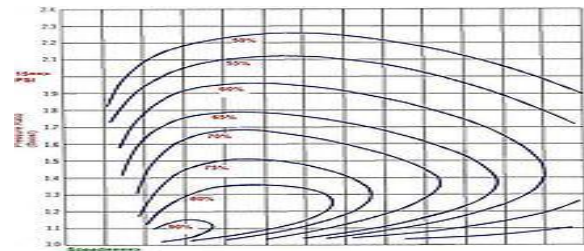


Figure 1.2 nomogram of efficiency of rotary blower

In order to meet customers concern related to its performance due to prevailing flow distribution inside the rotary blower, a detailed analytical study for two lobe configuration are reported. The study described is related to multi-recompression heater embodied as a modified roots compressor, wherein leakage effect was investigated. With the help of this research study, comprehensive numerical model dealing with flow simulation in the rotary blower comprises three lobes for an application to compressor was investigated. In this work numerical techniques were employed to determine flow characteristics for different orientation of rotors placed in the blower casing. The unsteady simulation of roots blower as a function of different angles indicates fluctuations of air velocities in the casing around lobes will have significant effect on estimation of exhaust rate. However, with rapid computer development in numerical simulation using Computational Fluid Dynamic (CFD) techniques, several industrial components [7-10] were analyzed, whose results have provided valuable insights for design improvement.

1.2 Working Principle

Twin Lobe Rotary Air Blowers belong to the category of Positive Displacement Blowers. They consist of a pair of lobes, rotating inside a properly shaped casing, closed at ends by side plates. The

drive to be is connected to the driven lobe, through a pair of gears and they always rotate in opposite directions. As the rotors rotate, air is drawn into inlet side of the cylinder and forced out the outlet side against the system pressure. With each revolution, four such volumes are displaced. The air which is forced out is not allowed to come back due to the small internal clearance within the internals of the machine except a very small amount called 'SLIP'. There is no change in the volume of the air within the machine but it merely displaces the air from the suction end to the discharge end, against the discharge system resistance. Lobe pumps are similar to external gear pumps in operation in that fluid flows around the interior of the casing. Unlike external gear pumps, however, the lobes do not make contact.

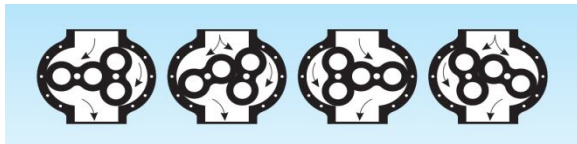


Figure 1.3 Working of lobe rotor

Lobe contact is prevented by external timing gears located in the gearbox. Pump shaft support bearings are located in the gearbox, and since the bearings are out of the pumped liquid, pressure is limited by bearing location and shaft deflection. As the lobes come out of mesh, they create expanding volume on the inlet side of the pump. Liquid flows into the cavity and is trapped by the lobes as they rotate. Liquid travels around the interior of the casing in the pockets between the lobes and the casing -- it does not pass between the lobes. Finally, the meshing of the lobes forces liquid through the outlet port under pressure.

1.3 Problem Statement

The rotary blowers are so rugged machines which are noisy and inefficient in nature. In general, the noise levels are more than 110 dB, and the efficiency is

less than 65% level. Moreover, the characteristic curves run very steep (Figure 1.2) i.e., nearly constant volume flow is produced over a wide range of pressure ratio. Thus, to control the flow rates at the same pressure ratio is difficult and requires design changes in lobes/rotors profiles. To troubleshoot or overcome these problems, measurements at plant site or prototype test results through scale down experiments at laboratory are not only complex task in terms of money and time but also will not yield expected flow characteristics that will aid to improve performance of component. Alternatively, the flow inside the rotary blower/pump also known as roots blower can be obtained through computational fluid dynamics techniques.

1.4 Methodology

Due to unavailability of factory dimensions existing model of lobe rotor was imported in altair hypermesh software from public domain. This model as IGES file comprises surfaces, splines, points imported to preprocessor Hypermesh for fluid portion extraction. On its import the model surfaces are grouped into different type collectors. After importing the pump assembly extraction of fluid portion (rotors along with casing and inlet/outlet pipes).

Due to presence of small clearances of the order ~2-3 mm between lobe to wall and lobe to lobe, domain discretization with hexahedral elements are made to capture flow in the clearance regions.

2. Impeller Geometry

The Roots compressor has a two-lobe design for the impellers. The two-lobe design has a high volumetric displacement. Figure 2.1 shows the actual shape of the impeller in the Roots compressor, called the "design shape" (solid line). Another shape called the "base shape" is defined which has a circle-involutes-circle profile (dashed line). Mathematical equations

are first derived for the “base shape” and are then modified to arrive at the equations of the “design shape.”

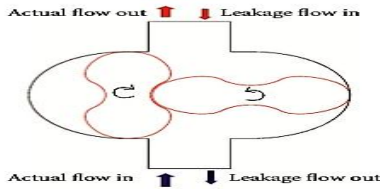


Figure 2.1 Schematic of a two-lobe Roots-type multi-recompression

For $\theta = [0, \beta_1]$,

$$x_1 = R_1 \cos\left(\pi - \frac{5\theta}{4}\right) + x_0,$$

$$y_1 = R_1 \sin\left(\pi - \frac{5\theta}{4}\right) \quad 1$$

For $\theta = [\beta_1, \beta_2]$,

2.1 Base shape

If we consider the first quadrant the involute profile shown in Figure 2.2 is a combination of three arcs: the mouth (or waist) and upper portion of the lobe are circular (R_1 and R_2) and the convex arc connecting them is an involute, which is formed by tracing the end of the string unrolling from the base circle (R_b). The current profile is created with the following parametric equations for the waist, involute and upper lobe shapes.

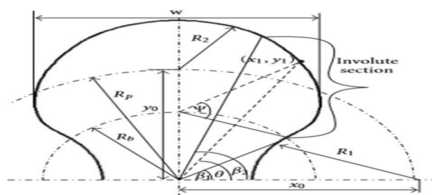


Figure 2.2 Base shape of rotor blade

$$x_1(\theta) = R_{21}(\psi) \cos(-\beta_1) + R_{22}(\psi) \sin(-\beta_1)$$

$$y_1(\theta) = R_{22}(\psi) \cos(-\beta_1) - R_{21}(\psi) \sin(-\beta_1), \quad 2$$

$$R_{21}(\psi) = R_b \{ \cos \psi + \psi \cdot \sin \psi \},$$

$$R_{22}(\psi) = R_b \{ \sin \psi - \psi \cdot \cos \psi \}. \quad 3$$

The angle “ ψ ” goes from 0° to 86.4708° when θ goes from 40° to 70° . The relation between ψ and θ is as follows:

$$\theta = \tan^{-1} \left(\frac{\sin \psi - \psi \cdot \cos \psi}{\cos \psi + \psi \cdot \sin \psi} \right). \quad 4$$

For $\theta = [\beta_2, \pi/2]$,

$$x_1(\theta) = R_3 \cos \left(\frac{52.6\pi(\theta - \beta_2)}{180(\pi/2 - \beta_2)} + 37.4\pi/180 \right),$$

$$y_1(\theta) = R_3 \sin \left(\frac{52.6\pi(\theta - \beta_2)}{180(\pi/2 - \beta_2)} + 37.4\pi/180 \right) + y_0 \quad 5$$

The values shown in Figure 1.33 are as follows (inches for linear dimensions and radians for angles):

$R_1 = 1.44$, $R_b = 0.8$, $R_p = 1.787$, $R_3 = 1.37$, $x_0 = 2.255$, $y_0 = R_p = 2.239$, $\beta_1 = 4\pi/18$, and $\beta_2 = 7\pi/18$.

By substituting the above values in (1)–(5), it is found that the lobe is 3.119 inches wide. The design shape is a modification of the base shape. To adjoin the “add-ons” to the involute curve, the normal to the involute curve has to be found. To find the normal to the involute at any point, the gradient (slope) of the normal is first found out by taking negative reciprocal of dy/dx ,

$$\frac{-1}{dy/dx} = m = \frac{\sin \psi \cdot \sin \beta_1 - \cos \psi \cdot \cos \beta_1}{\sin \psi \cdot \cos \beta_1 + \cos \psi \cdot \sin \beta_1} \quad 6$$

The thickness of add-ons is “ a ” = 0.04115 in. Hence, the extra material added will be

$$X_{add} = a \cdot \cos(\tan^{-1} m)$$

$$Y_{add} = a \cdot \sin(\tan^{-1} m) \quad 7$$

We add this to the x and y coordinates of the “base shape.” Hence,

$$X_{design} = x_1(\theta) + X_{add},$$

$$Y_{design} = y_1(\theta) + Y_{add}. \quad 8$$

$$x_1(i), y_1(i)$$

$$x_2(j), y_2(j) \quad 9$$

For the “tip strip” a value of 0.055 is added for $\theta = 89.444^\circ$ to 90° . This is the angle where the tip strip starts and is obtained from the machine drawing of the “design shape.”

3. Experimental Methodologies

3.1 Computation Fluid Dynamics

Computational fluid dynamics (CFD) is a branch of fluid mechanics that uses numerical analysis and data

structures to solve and analyze problems that involve fluid flows. The design of turbo machinery components such as fans, blowers and pumps are based on empirical formulae

3.2 Description of lobe pump

Figure 3.1 shows typical rotary positive displacement with its end covers removed. The drive shaft is connected to drive shaft through a pair of helical gears at the rear end. The drive shaft front end is connected to an electric motor drive using a belt drive arrangement. The lobed shafts rotate with equal rotational speed in opposite directions. The bearings and gears are splash lubricated by oil filled in the end cover chambers.

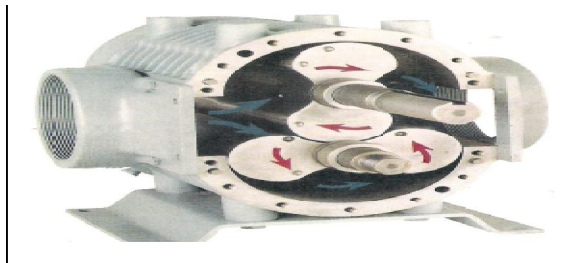


Figure 3.1 rotary positive displacement pumps without end cover

For requirements of pressure rise at blower discharge, the drive shaft rotates in an anti-clock wise direction (viewed from drive end). The direction of blower shaft is reversed for suction pressure requirements. The gas handled by such blower is oil free as the gas path is not coming into contact with lubricating oil circuit. The axes of the drive and driven lobes are set at right angles and working clearances between lobes, casing and the side plates. In one working period, the rotors rotate in a reverse direction; the fluid is compressed and transported from the inlet to the outlet via the chamber.

As soon as the impeller passes the breakaway point, the gas in the well mixes with the gas in the blower casing. After multiple rotations, pressure starts building up in the outlet region and a blower casing is

developed. This causes leakage gas to flow back into the low-pressure region through the clearances. The leaked gas, being at a high-temperature, heats the incoming gas. The volume of the incoming gas increases, decreasing the volumetric efficiency and hence reducing the mass flow rate significantly.

3.3 CAD Modal Lobe Pump

Three dimensional solid model was generated using the dimensions in front/top and side views of several part and assembly drawings using industry standard CAD modeler commercial software package. This model as IGES file comprises surfaces, splines points are exported to another preprocessor Hypermesh for fluid portion extraction. On its import the model surfaces are grouped into five groups as shown in Figure-3.2. Since the lobes rotating counter clockwise direction and it is essential to consider orientation at 15 degrees. This involves lot of simulation and pre-processing work and the present report is considered only two orientations wherein rotors are at 180- 90 Figures 3.3.

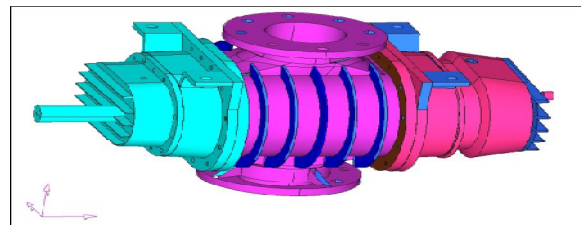


Figure 3.2 Imported model of lobe rotor

In order to account fluid passage due to change of lobes rotation at 45° , the lobes are rotated about its pivot point in center in x direction.

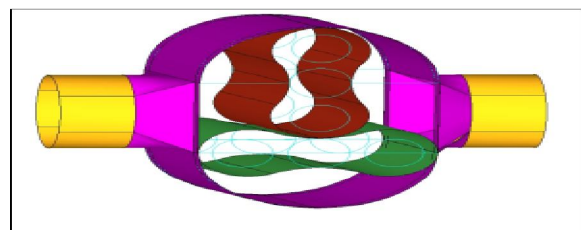


Figure 3.3 Lobe rotors at 180-90 orientation

The model for roots blower with the rotating lobes connecting suction and discharge duct is shown in

Figure-3.4. In order to carry out compute pressure and velocities of entrained air when the lobes are subjected rotations, flow passage has to be discretized with computational mesh comprises different types of elements. Using above surface model, with the closure of inlet and exit duct end faces, volume can be generated filled with tetrahedral elements. In order to account fluid passage due to change of lobes rotation at 45° , the lobes are rotated about its pivot point in center in x direction.

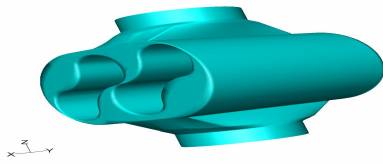


Figure 3.4 Roots blower connecting suction and discharge duct.

3.4 Computational Grid Generation

At the core of CFD, computational grid is central element, which often considered as most important and time consuming part in simulation projects. The quality of the grid plays a direct role on the quantification of flow results, regardless of the flow solver used for simulation..

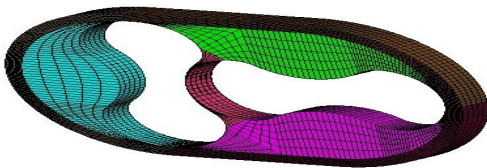


Figure 3.6 hexahedral mesh for one end of the lobe pump

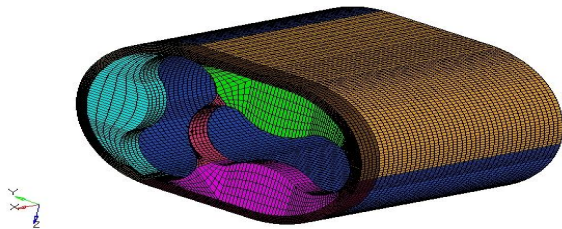


Figure 3.7 Mesh element of casing region

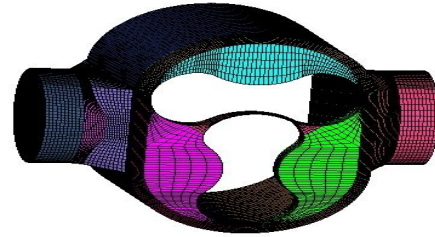


Figure 3.8 mesh continuity with inlet and exit pipes

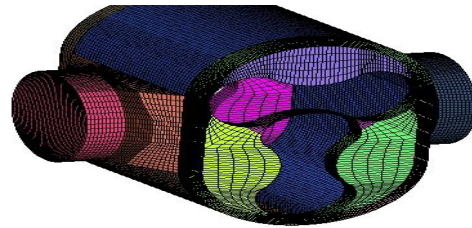


Figure 3.9 solid mesh of lobe pump block

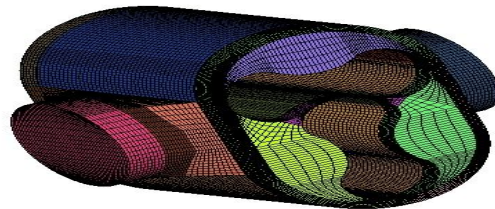


Figure 3.10 mesh generation of complete element

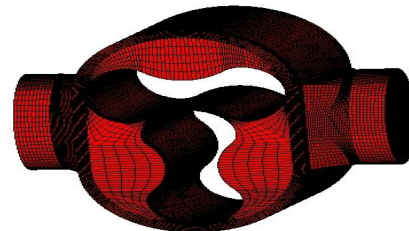


Figure 3.11 grid generation of lobe rotor

With the help of above grid, boundary conditions like inlet, exit, rotating wall1 and rotating wall2 are created. The main grid collectors with these boundary conditions regions shown in Figure 3.12 with appropriate solver deck can be exported for flow simulation.

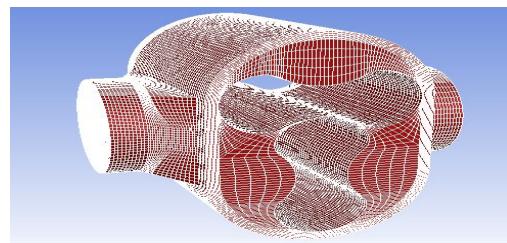


Figure 3.12 grid collectors with boundary condition

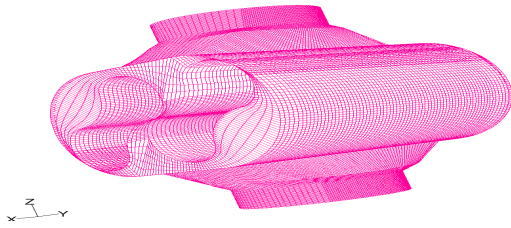


Figure 3.13 Orientation of lobes in 45 degrees position
After exporting the mesh into the flow solver, the working fluid will be ideal gas, compressible, steady, three dimensions. The several plane slices in x direction of computational domain provides valuable flow results. `

3.5 Selection of Flow Solver

ANSYS Fluent is a state-of-the-art computer program for modeling fluid flow, heat transfer, and chemical reactions in complex geometries.

However the input to the solver must be grid file saved as .cas file. The software can be activated by double clicking the .case file in the relevant directory. It reads geometrical information and checks the grid quality for negative volume displays the mesh along with boundary conditions regions as shown in Figure 3.19

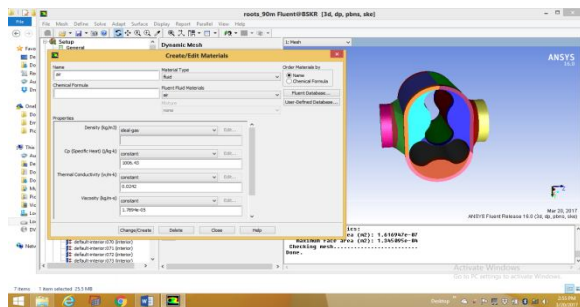


Figure 3.19 mesh generation with geometrical condition

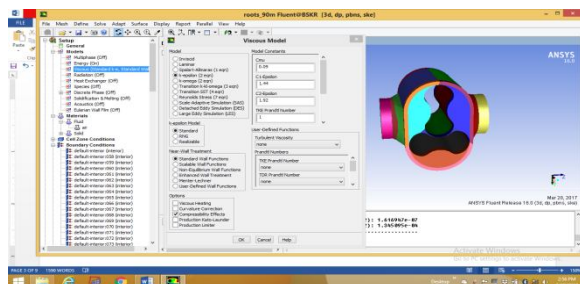


Figure 3.20 selection of available model on viscosity

In order to see the results are computed in right direction, using report mass flow flux values of at inlet and outlets are computed and shown below.

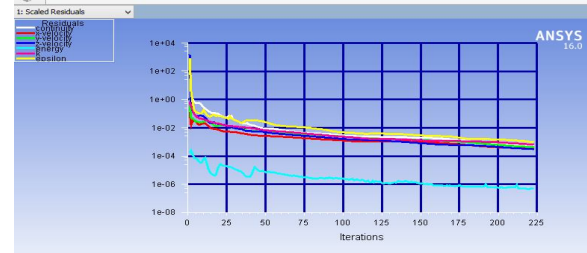


Figure 3.21 Scale residuals graph with rotors perpendicular

In order to see the results are computed in right direction, using report mass flow flux values of at inlet and outlets are computed and shown below

Mass Flow Rate	(kg/s)
inlet	0.18000001
exit	-0.18018808

In order to carryout flow analysis in the lobe pump, wherein the rotors are reoriented to 45 degrees are modeled geometrically and generated the computational mesh. The mesh along with inlet, exit, rotating walls are format output of equation residuals exported to fluent solver as shown in the exported format output of equation residuals exported to fluent solver .

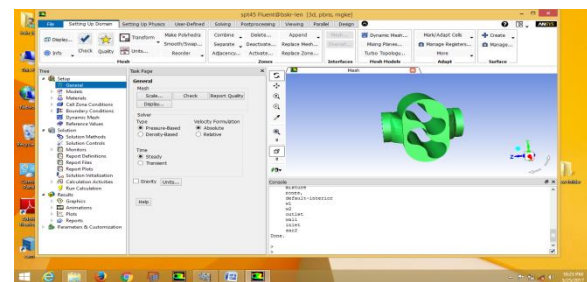


Figure 3.22 mesh element exported to fluent solver

After checking the mesh quality, scaling, materials like compressible air ideal gas has been considered whose working pressure is 1 atm. To capture viscous losses, Reynolds Average Navier Stokes two equation turbulence model with standard wall function are considered

For the rotating walls, in the boundary condition wall motion is selected as moving with rotational speed 272.2 Rad/sec whose screen shot is shown in the Figure 3.23. .

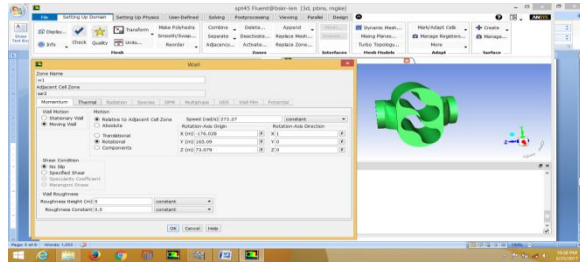


Figure 3.23 Boundary conditions for rotating walls

At the inlet of lobe pump total gauge pressure 40 Pascal's are prescribed and exit 40000 Pascal normal to boundary are assigned. For the rotating walls, in the boundary condition wall motion is selected as moving with rotational speed 272.2 Rad/sec whose screen shot is shown in the Figure 3.23. The second rotor is rotating in anti-clockwise direction whose rotational speed is assigned as -272.2 Rad/sec. Under these conditions, after initialization the governing equations, three momentum, two turbulence, continuity and energy equations are iterated to meet convergence criteria The graphical output of equation residual error over iterations are shown in Figure 3.24

The Flux of mass flow across inlet and exit locations are computed and shown below ensures the conservation of mass principle.

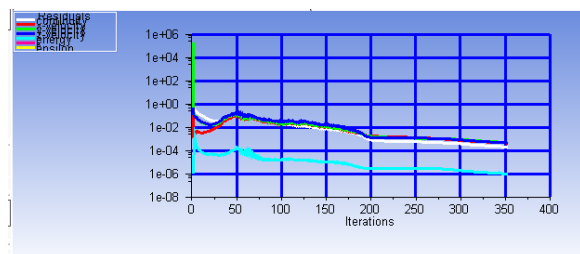


Figure .3.24 graphical output of residual error over iteration

It is observed in the case of rotational wall, the convergence of governing equations is slower than non-rotating case.

Mass Flow Rate (kg/s)

Inlet	1.4629610
Outlet	1.4621507

Using the surface integrals, with the mass flow average, absolute pressure across the inlet and exit locations are calculated as - Mass-Weighted Average

Absolute Pressure (Pascal)

Inlet	100167.22
Outlet	138265.83

4. Results and discussions

4.1 Vector plots

The Velocity vectors in the middle plane of lobe pump obtained in the case of rotors oriented 180 and 90 degrees positions are shown in the Figure 4.1

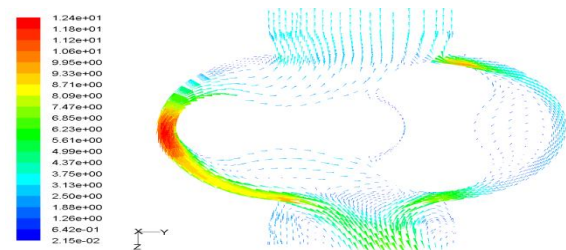


Figure 4.1 Velocity vector in middle plane at 180-90 position

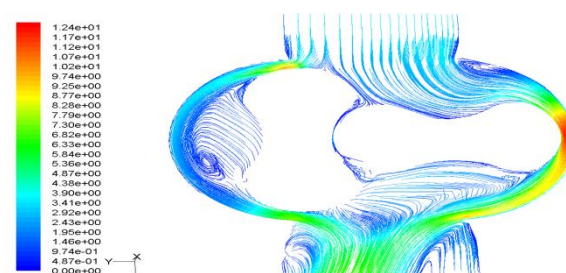


Figure 4.2 Flow circulations at the inlet with strong turbulent vortices

4.2 Flow contour

4.2 Flow contour

This is a case of assumption that the rotors are under stationary conditions, mass flow at inlet is 0.18 kg/s and exit pressure is 40530 Pascal. The velocity

vector from inlet in the lobe pump chamber is uniform and exhibits high magnitudes at the end of rotor positioned at 180 degree. The flow at the inlet also indicates quite strong turbulent vortices whose effect in the form of flow recirculation can be visualized in Figure 4.2. Being the flow is compressible the velocity Mach contours and pressure are detailed in the Figures 4.3 and 4.4

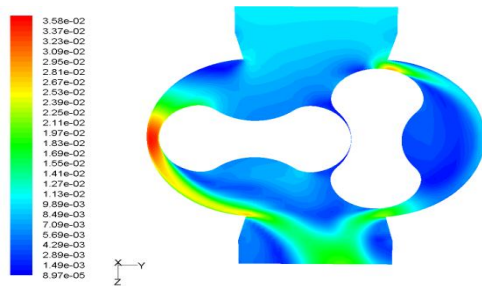
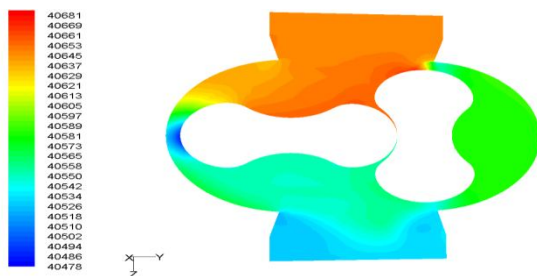


Figure 4.3 Velocity Mach contour

The Mach number variation the lobe pump plane indicates high at the location of rotor positioned at 0 degrees. As a result the Mach number exhibits high at most part of inlet location.

The pressure plot in the form of contours are generated in the lobe pump middle plane and its variation from inlet accelerates and becomes low pressure at the rotor positioned at 0 degrees and then increases at its upper surface.



The pressure plot in the form of contours are generated in the lobe pump middle plane and its variation from inlet accelerates and becomes low pressure at the rotor positioned at 0 degrees and then increases at its upper surface. This implies that pump is attaining high pressure at the exit location. The

numerical results obtained for several flow parameters are visualized in the computational domain using solver post-processor. The velocity vector in the mid-plane of the blower is shown in the Figure -4.5.

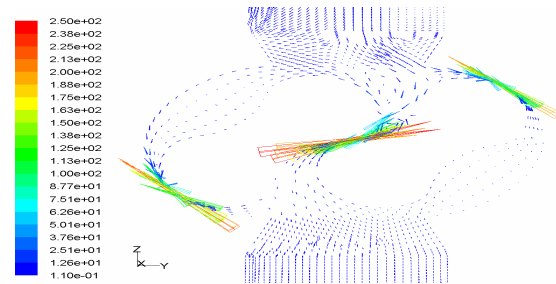


Figure 4.5 velocity vectors at mid plane of blower

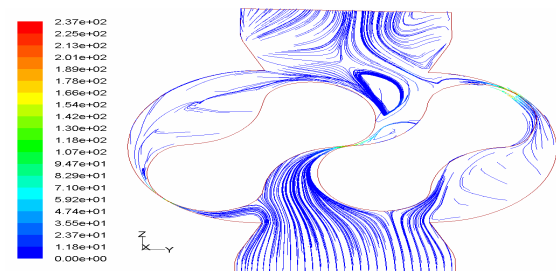


Figure 4.6 Stream line pattern of leakage flow in mid plane. The leakage flow starts from the discharge side of the blower and flows towards blower inlet. The mass averaged flow rate at inlet region is 0.14 kg/sec. Maximum velocity 13 m/sec occurs in the clearance region between drive lobe and casing. Figure-4.6 shows the stream line pattern of leakage flow in the mid plane. The flow recirculation can be seen at inlet and outlet

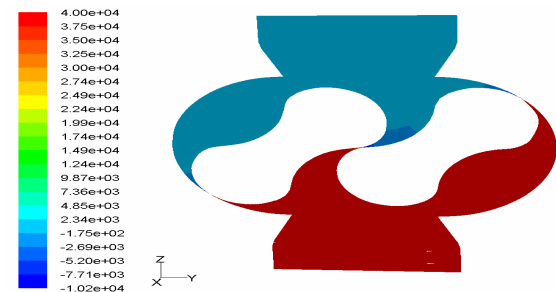


Figure 4.7 pressure variation in middle plane of root blower

Passage near the rotors and clearance area between drive lobe to casing, and also at exit location. Figure 4.7 shows the pressure variation in the middle plane of the blower the contours of maximum pressure are observed at the outlet region whereas the inlet region has lower pressure. The minimum pressure occurs in the clearance between drive lobe and casing.

4.3 Summary of Results

The summary of results obtained from the present cfd analysis is as follows

No	Mass average quantities	Inlet	Outlet
1	Flow Rate Kg/sec	0.13450293	0.134446
2	Static Pressure Pa(gauge)	19.988194	111.90541
3	Velocity m/sec	4.8759556	3.6270936
4	Total pressure Pa (gauge)	35.071281	119.97011
5	Temperature Degree K	309.69043	309.99295
6	Density Kg/m**3	.1400392	.11399997

5. Conclusion and future scope of work

5.1 Conclusion

The rotary device comprises counter-rotating lobes used in Circulating Fluidized Bed Combustion based Power Plant concerns reduction in volumetric efficiency and generation of excessive noise due to leakage of flow/unequal velocity distribution. It has also several applications in process and petro-chemical industries. To troubleshoot or overcome these problems, measurements at plant site or prototype test results through scale down experiments at laboratory are not only complex task in terms of money and time but also will not yield expected flow characteristics that will aid to improve performance of component. Alternatively, the flow inside the rotary blower/pump also known as roots blower can be obtained through computational fluid dynamics techniques.

Accordingly, the assembly of this blower has been studied and a solid model was created. Flow passage of suction, discharge, casing comprises lobes are extracted. Due to presence of small

clearances of the order ~2-3 mm between lobe to wall and lobe to lobe, domain discretization with hexahedral elements are made to capture flow in the clearance regions. The volume mesh has imported to flow solvers to simulate compressible flow in steady state to study the leakage flow and pressure fluctuations. With the flow/thermal conditions such inlet stagnation pressure, exit static pressure, lobe rotations, etc., leakage mass flow rate and pressure fluctuations was obtained through three dimensional flow simulation.

Two cases have been analyzed keeping in view of difficulties for numerical simulation - first one is the rotors are positioned 0 and 90 degrees which are treated stationary state. For the inlet and exit pressure conditions, the velocity vectors exhibits high at the rotor positioned at 0 degree and its variation at inlet generates severe turbulent vortices. The absolute pressure at the middle plane of the lobe pump generates high at exit locations indicating that it acts like a pressure rise application. In case of rotating walls rotating in counter clock wise direction, the pressure drop across the blower inlet and exit locations are found to be 92 Pascal The simulation predicts the maximum velocity of 6 m/sec in the clearance between lobe and casing. The leakage flow rate calculated from the mass averaged values of velocities and density of flow medium is found to be 0,135 kg/sec. Compressible ideal flow simulation has been carried out for evaluation of leakage flow rates and volumetric efficiencies.

5.2 FUTURE SCOPE OF WORK

The Roots type supercharger shown below is used to boost the intake pressure of an internal combustion engine by approximately 12-15 PSI, drastically improving the performance of the engine. The device consists of two rotor assemblies turning

in opposite directions. The air is pushed around the outside of the rotors and out the bottom. The outer surface of each rotor lobe contains a Teflon seal strip to prevent leakage. In order to reduce pulsing of the pressure, the lobes are often twisted along the rotational axis, or helically, as shown Figure 5.1

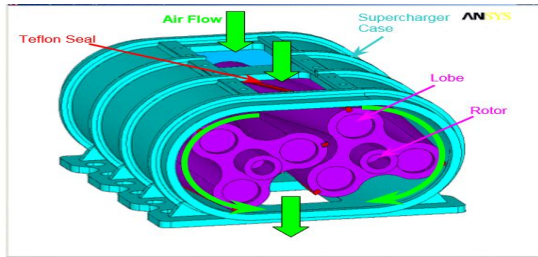


Figure 5.1 Lobe rotors with three lobes and supercharger case

One of the future scopes of for this class of problem is to determine the clearance or interference of the rotor lobe seals and the case. Minimizing this clearance under start-up and operating temperatures is crucial to supercharger performance

REFERENCES

- 1.Rajaram S, Natarajan R, Design features and operating experience of BHELs First CFBC boiler installed at Sinarmas, BHEL Jnl, Vol 21 pp 58-66, 2000.
- 2.Iwao OHTANI and Tetsuo IWAMOTO, Reduction of Noise in Roots Blower, Bul. JSME, Vol. 24, No.189, 1991
- 3.G.Mimmi and P.Pennachi, Analytical model of a particular type of positive displacement blower Procs. of Institution of Mechanical Engineers, Vol 215 Part-C pp 517-526, 1999
- 4.David I. Blekhman, Joseph C. Mollendorf, James D. Felske, and John A. Lordi, Multi-Control-Volume Analysis of the Compression Process in a High-Temperature Root's Type (four lobes) Compressor, International journal of Rotating Machinery, 10: 45–53, 2004

- 5.Z.F.Huang and Z X Liu, Numerical Study of a Positive displacement Blower (three lobes), Procs of Institution of Mechanical Engineers, Vol. 233,Part-C, pp 2309-2316, 2009

- 6.Ashish M. Joshi et.al Clearance Analysis and Leakage Flow CFD Model of a Two-Lobe Multi-Recompression Heater , Intl. Jrnl of Rotating Machinery Article ID 79084, Pages 1–10, 2006

- 7.Bhasker C, Numerical simulation of turbulent flow in complex geometries used in power plants, International Journal- Advances in Engineering Software, UK Vol.33, pp 71-83, 2002.

- 8.Bhasker C., Flow Simulation in Industrial Cyclone Separator, International Journal – Advances in Engineering Software, UK, Vol 43, pp 220-228, 2010

- 9.Bhasker, C., Troubleshooting Steam Turbine Bypass Valves – Role of CFD as a key Analytical tool, Technical Torque, PVS Industrial Magazine, India, pp 20-24, May-June, 2010.

- 10.Bhasker, C., Hydraulic Control Valve Flow Simulation, Prediction of flow Pattern in Globe type Control Valve using CFD, Technical Torque, PVS Industrial Magazine, pp 14-21, July, Aug, 2010

- 11.Thomson, J.F et.al Numerical Grid Generation – Foundations and Applications, North Holland, Amsterdam, 1985

- 12.ShekarMajumdar Pressure based finite volume algorithm for viscous flow computation, Lecture Notes, CFD Advances and Applications, NAL, Bangalore, India, 1994.